Electrochemical Synthesis Wormcast-like Pd-based Polycrystalline High Entropy Aggregates for Methanol Water Co-electrocatalysis

Yaxing Liu[a,b*], Wenhao Ding[b], Jiaxin Liu[a,b], Guizhe Zhao[a,b], Weiyin Li[c] and Yaqing Liu[a,b*]

[a] Shanxi Key Laboratory of Functional Polymer Composites, North University of China, Taiyuan, 030051, P. R. China

[b] School of Materials Science and Engineering, North University of China, Taiyuan, 030051, P. R. China

[c] School of Electrical and Information Engineering, North Minzu University, Yinchuan, 750021, P. R. China

***Corresponding authors:**

Yaxing Liu

Shanxi Key Laboratory of Functional Polymer Composites, School of Materials Science and Engineering, North University of China, Taiyuan, 030051, P. R. China

Email: yaxingliu@nuc.edu.cn

Yaqing Liu

Shanxi Key Laboratory of Functional Polymer Composites, School of Materials Science and Engineering, North University of China, Taiyuan, 030051, P. R. China

Email: lyq@nuc.edu.cn

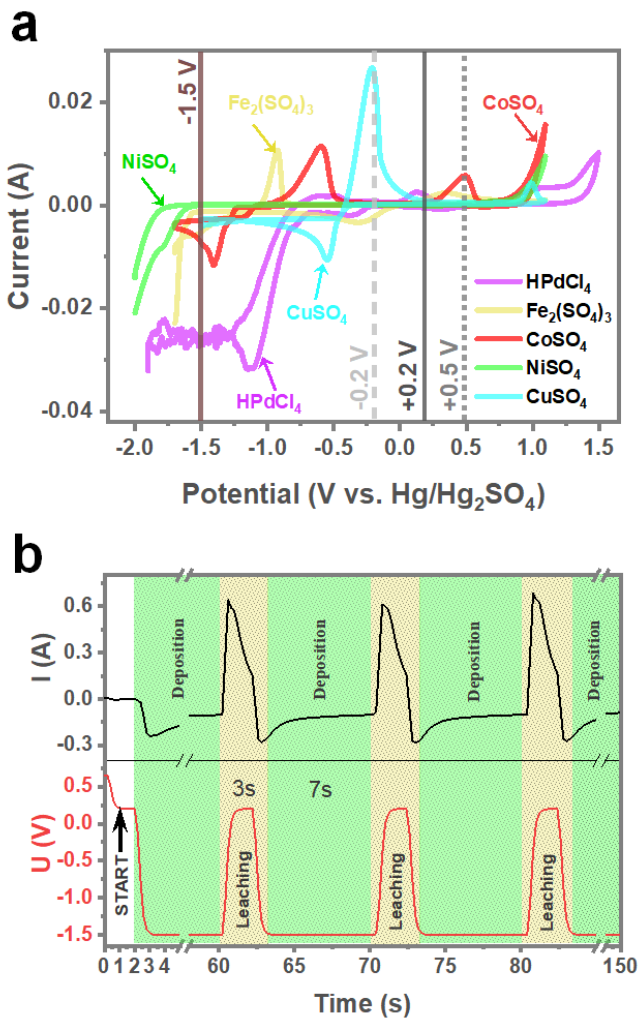

Figure S1. a) CV curves of Pd, Fe, Co, Ni, and Cu metal salts in 1 M Na_2SO_4 solution; b) Recorded data curves of current and voltage during the synthesis procedure.

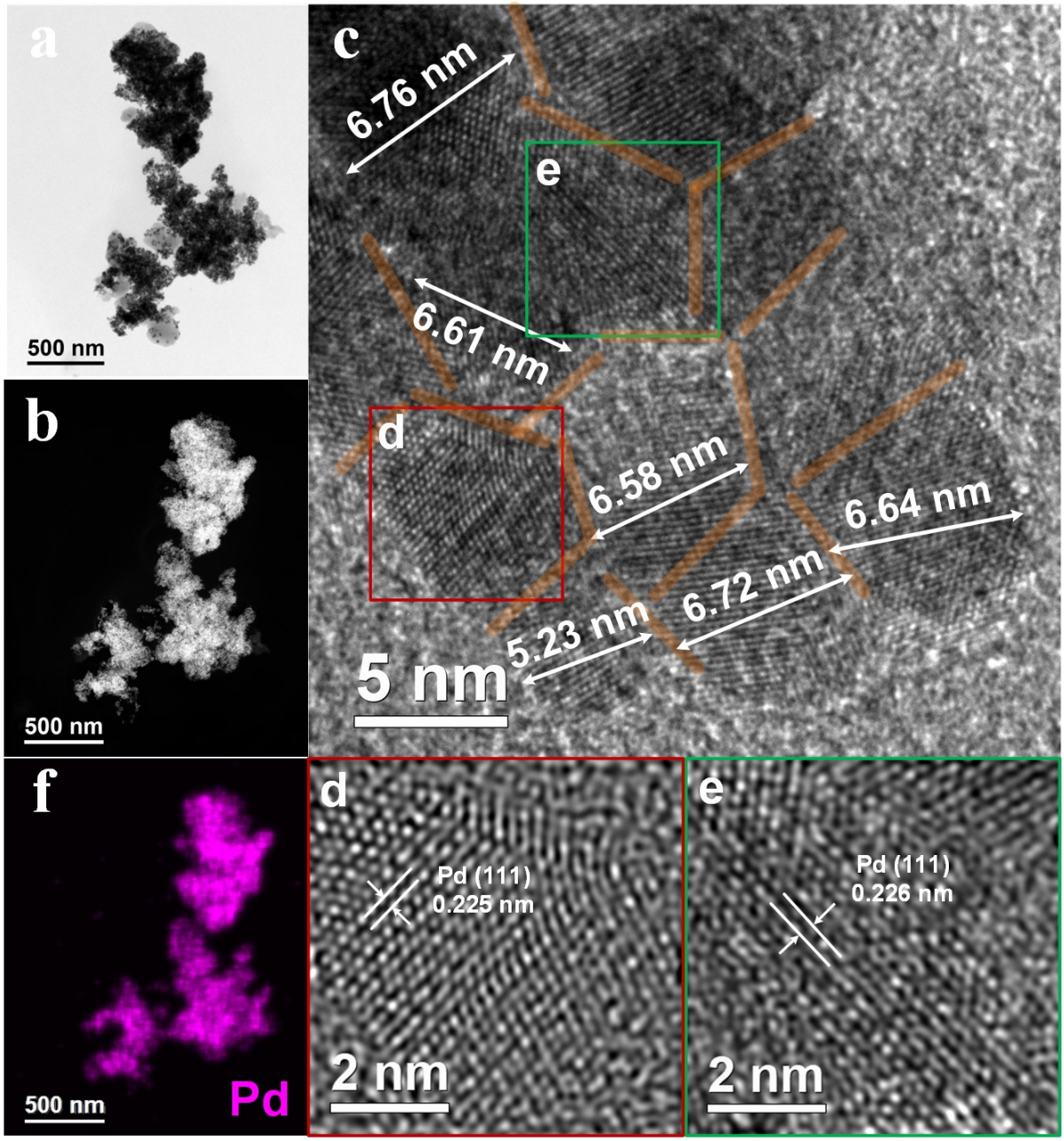

Figure S2. Morphology of Pd-Ns. a) SEM image; TEM images for a) bright-field and b) dark-field; c) HR-TEM image recorded from a selected region in image a); d, e) IFFT images according to the selected regions in image c); f) Elemental EDX mapping images.

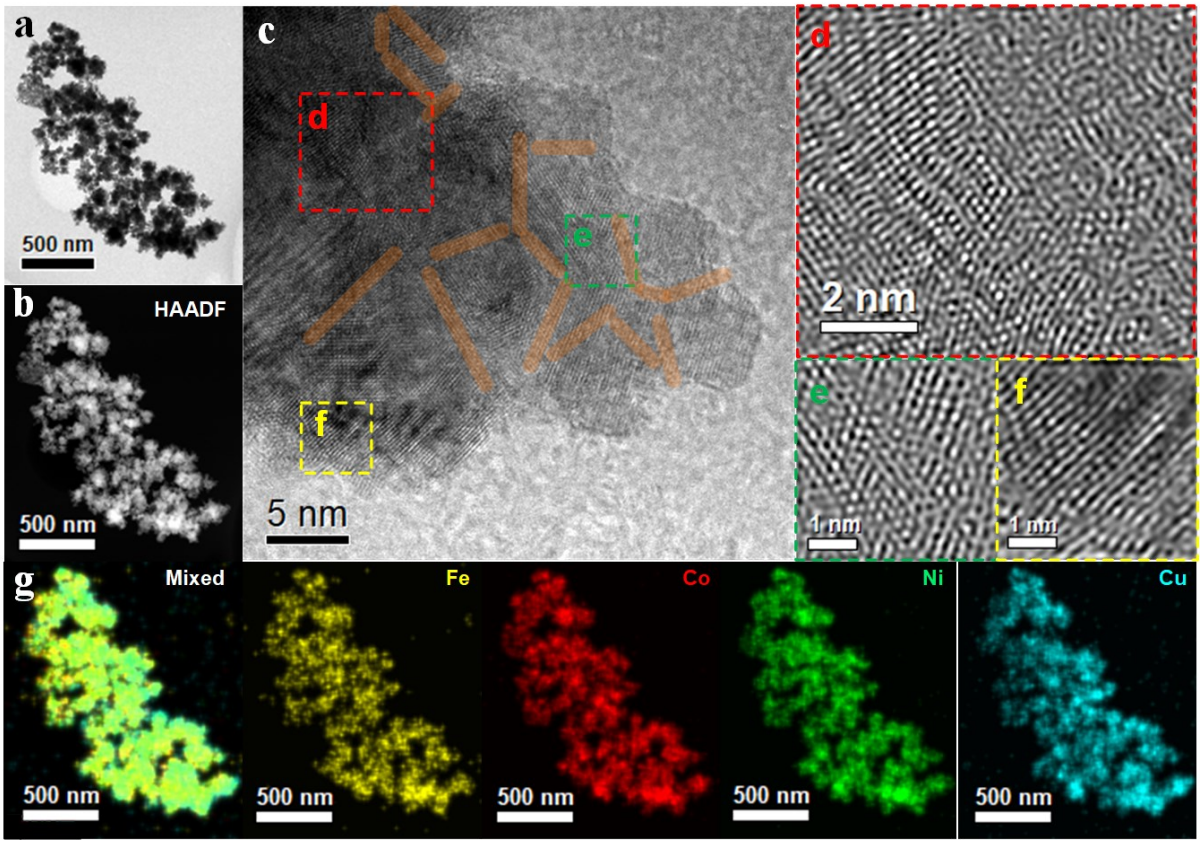

Figure S3. Morphology of FeCoNiCu-pHENs. a) SEM image; TEM images for a) bright-field and b) dark-field; c) HR-TEM image recorded from a selected region in image a); d, e, f) IFFT images according to the selected regions in image c); g) Elemental EDX mapping images.

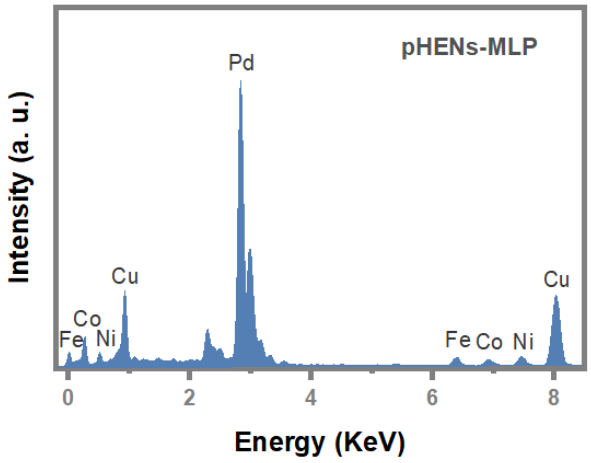

Figure S4. EDX spectra of PHENs-MLP.

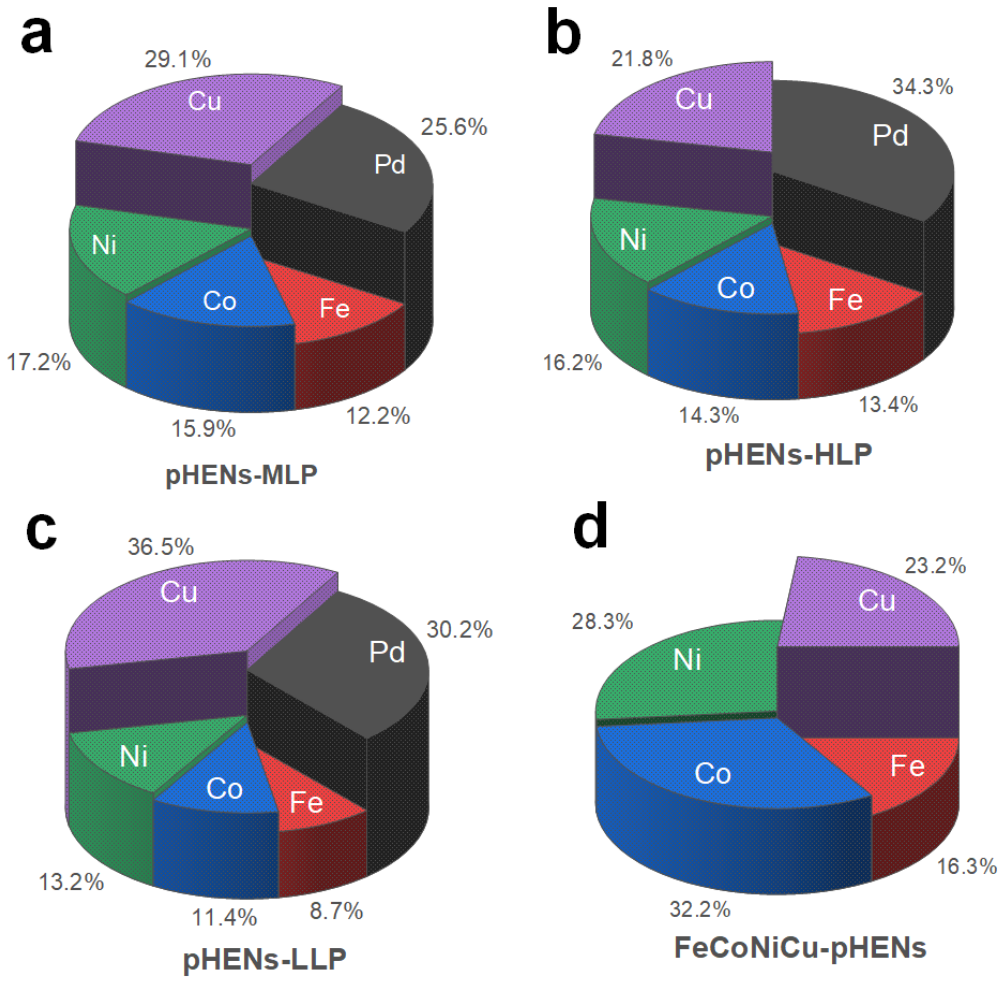

26

27 Figure S5. Element mass ratios of a) PHENs-MLP, b) PHENs-HLP, c) PHENs-LLP, and d) FeCoNiCu-pHENs.

28

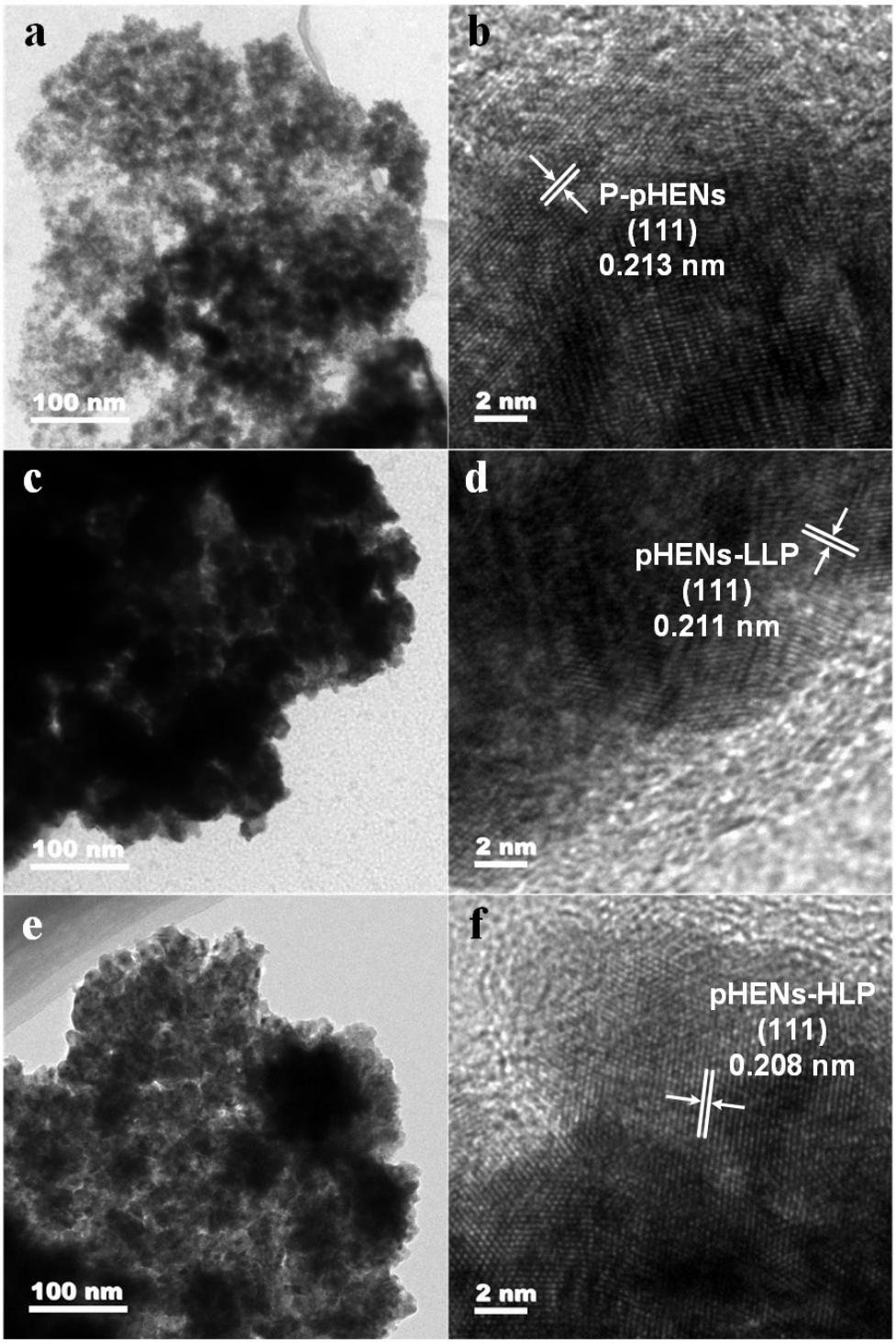

Figure S6 TEM images of a), b) P-pHENs, c), d) pHENs-LLP, and e), f) pHENs-HLP.

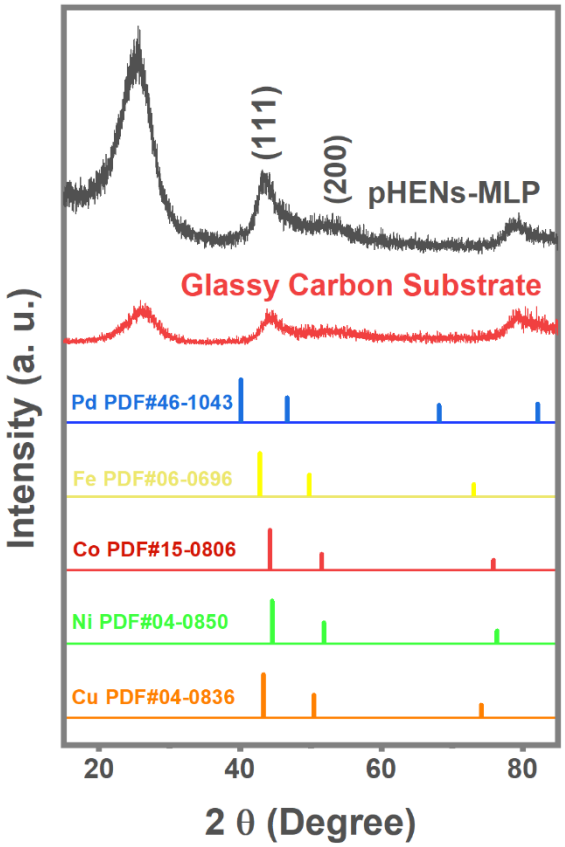

Figure S7. XRD patterns of PdFeCoNiCu-pHENs (pHENs-MLP) and glassy carbon substrate.

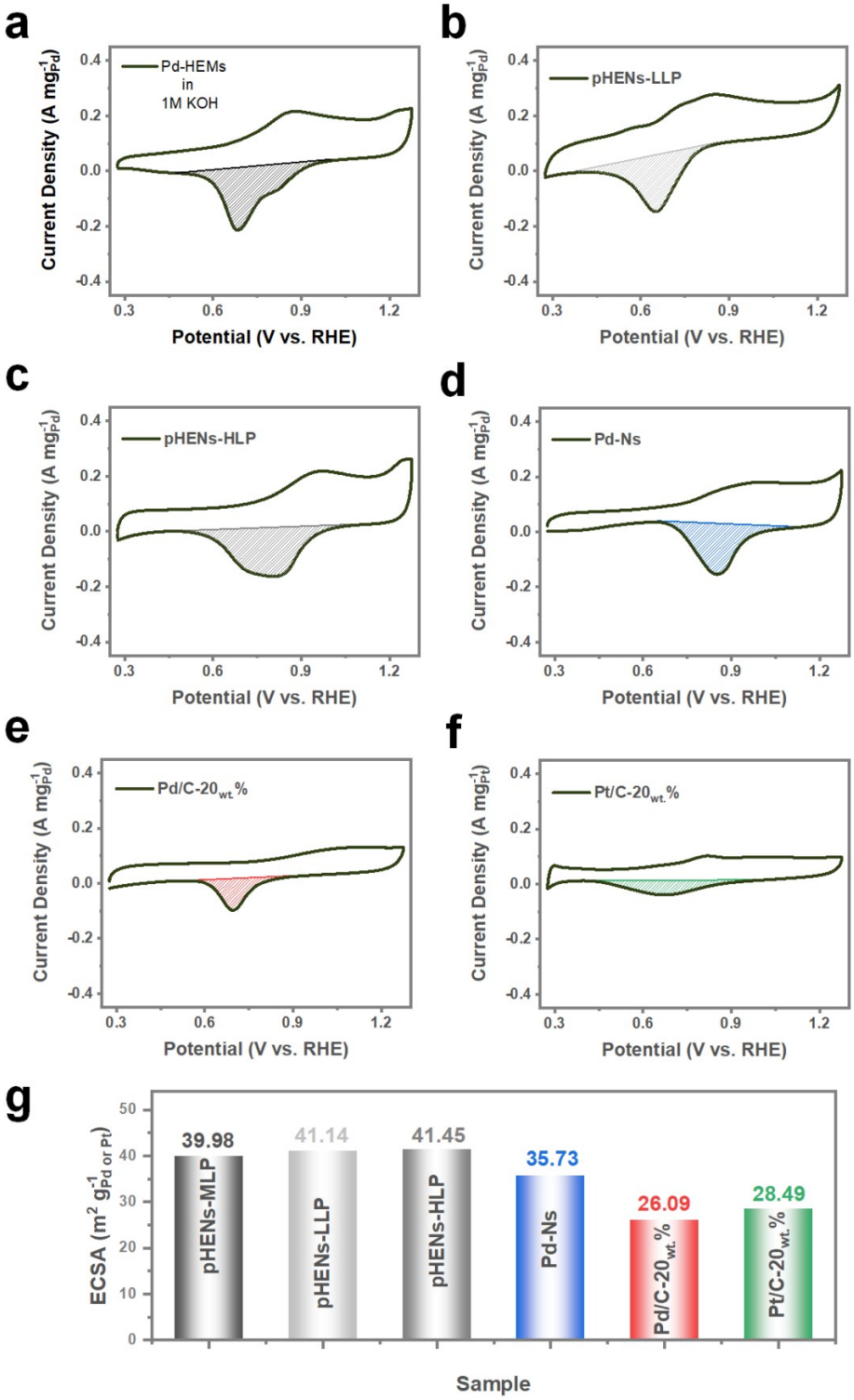

Figure S8. CV curves of samples were recorded in 1 M KOH solution. a) pHENs-MLP; b) pHENs-LLP; c) pHENs-HLP; d) Pd-Ns; e) Pd/C-20$_{wt.}$%; f) Pt/C-20$_{wt.}$%; g) corresponding ECSA of various samples.

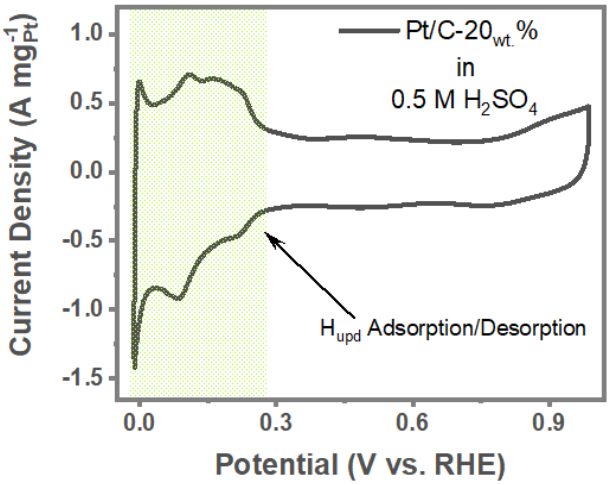

37

38 Figure S9. CV curve of Pt/C-$20_{wt.}$% was recorded in 0.5 M H_2SO_4 solution.

39

40

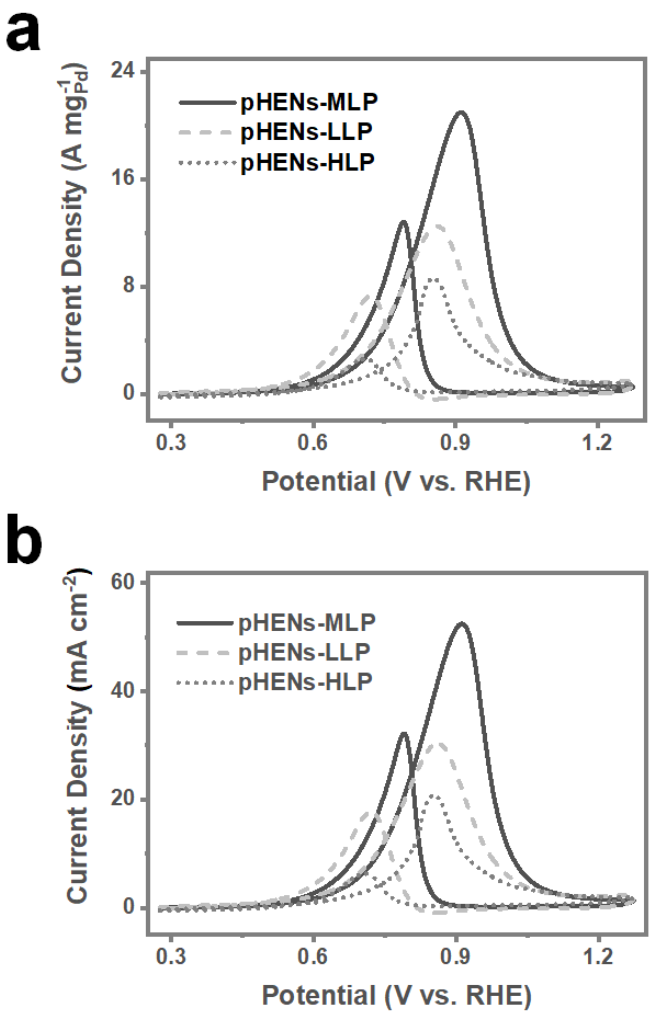

41

42 Figure S10. CV curves of PdFeCoNiCu-pHENs with different applied potentials in an N_2-saturated 1.0 M KOH

43 solution containing 1.0 M CH_3OH. a) Mass activity and b) specific activity toward MOR.

44

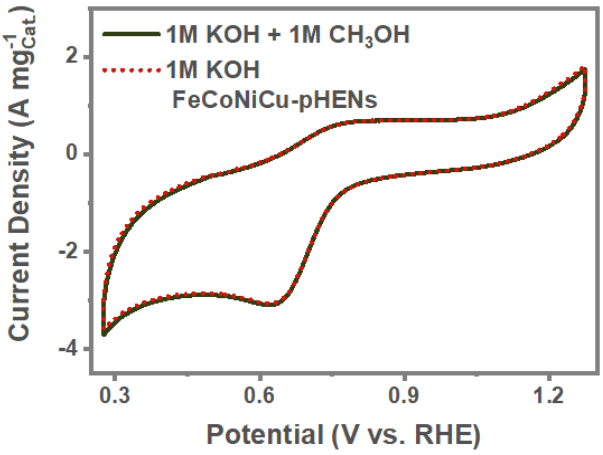

45

46 Figure S11. CV curves of FeCoNiCu-pHENs were recorded in N_2-saturated 1.0 M KOH solution mixing with

47 or without 1.0 M CH_3OH.

48

49

50

51

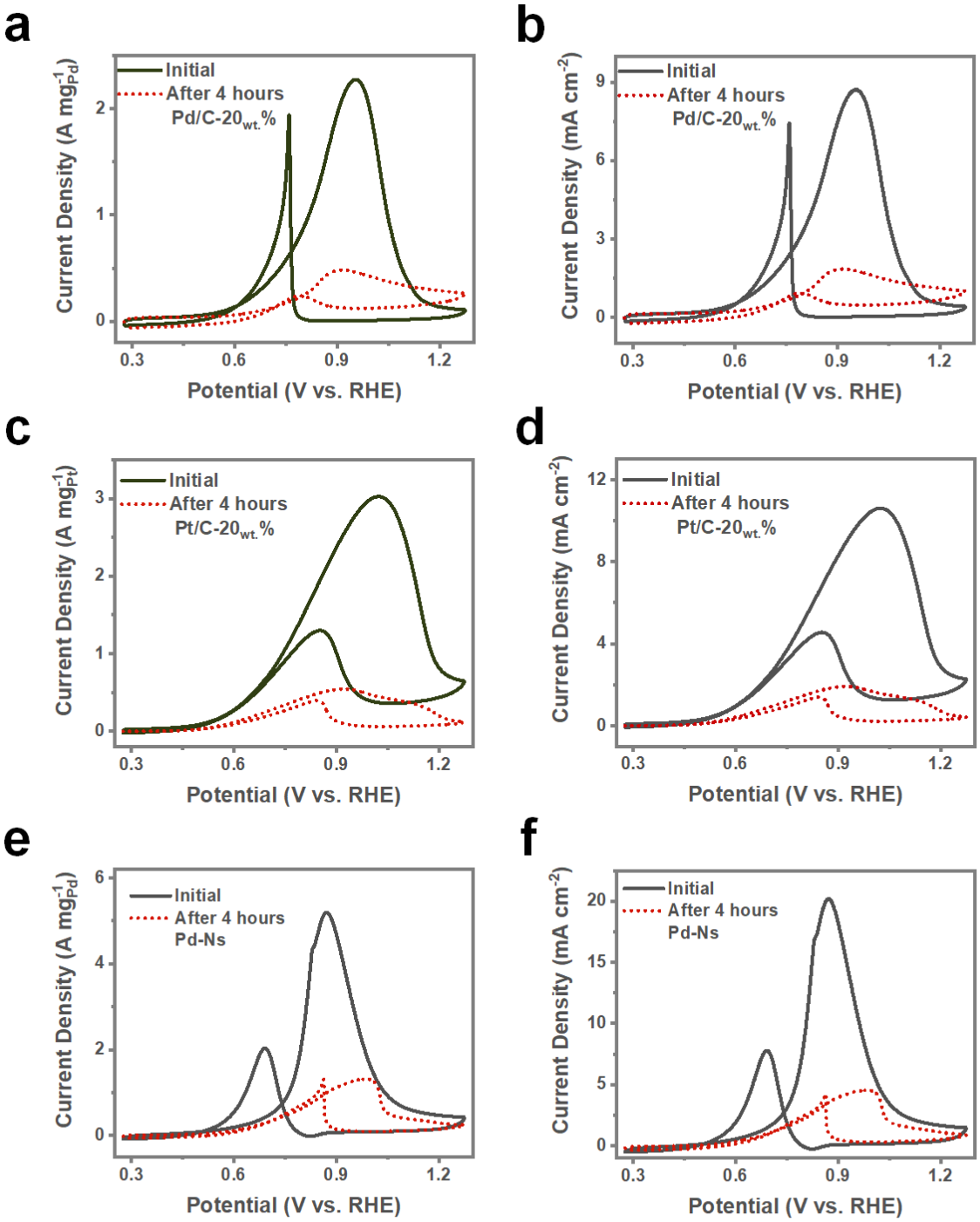

Figure S12. Mass activities of commercial catalysts before and after the chronoamperometric test. a) Mass and b) specific activity of Pt/C-20$_{wt.}$%; c) Mass and d) specific activity of Pd/C-20$_{wt.}$%; e) Mass and f) specific activity of Pd-Ns.

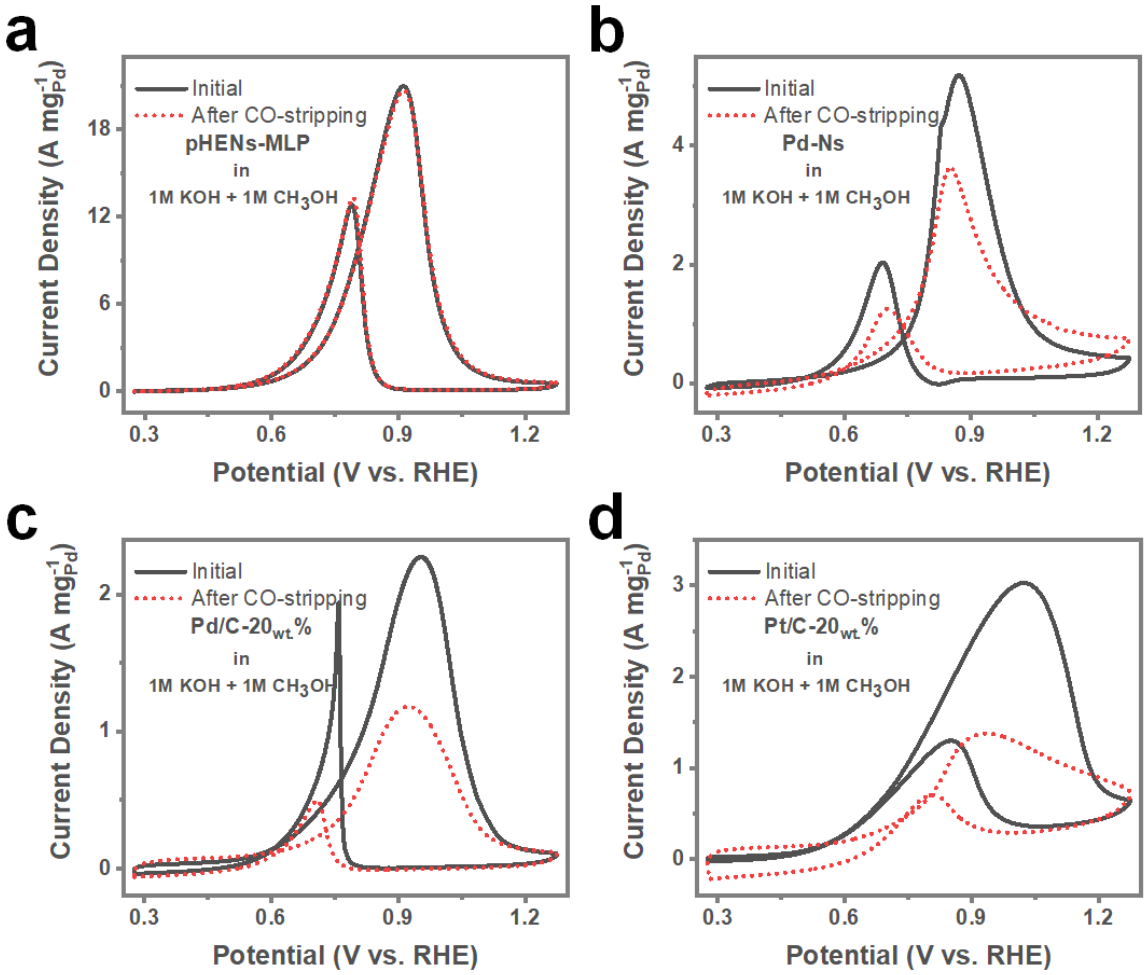

56

57 Figure S13. MOR electrocatalytic performances of a) pHENs-MLP, b) Pd-Ns, c) Pd/C-20$_{wt.}$%, and d) Pt/C-20$_{wt.}$%

58 before and after the CO-stripping test.

59

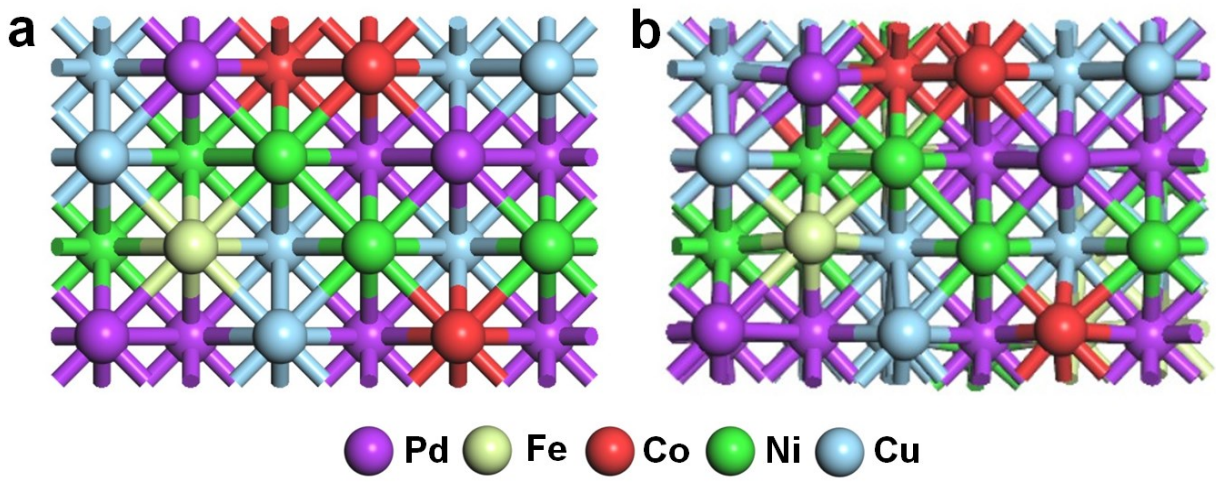

60

61 Figure S14. The calculated model of PdFeCoNiCu-pHENs a) before and b) after the structural optimization.

62

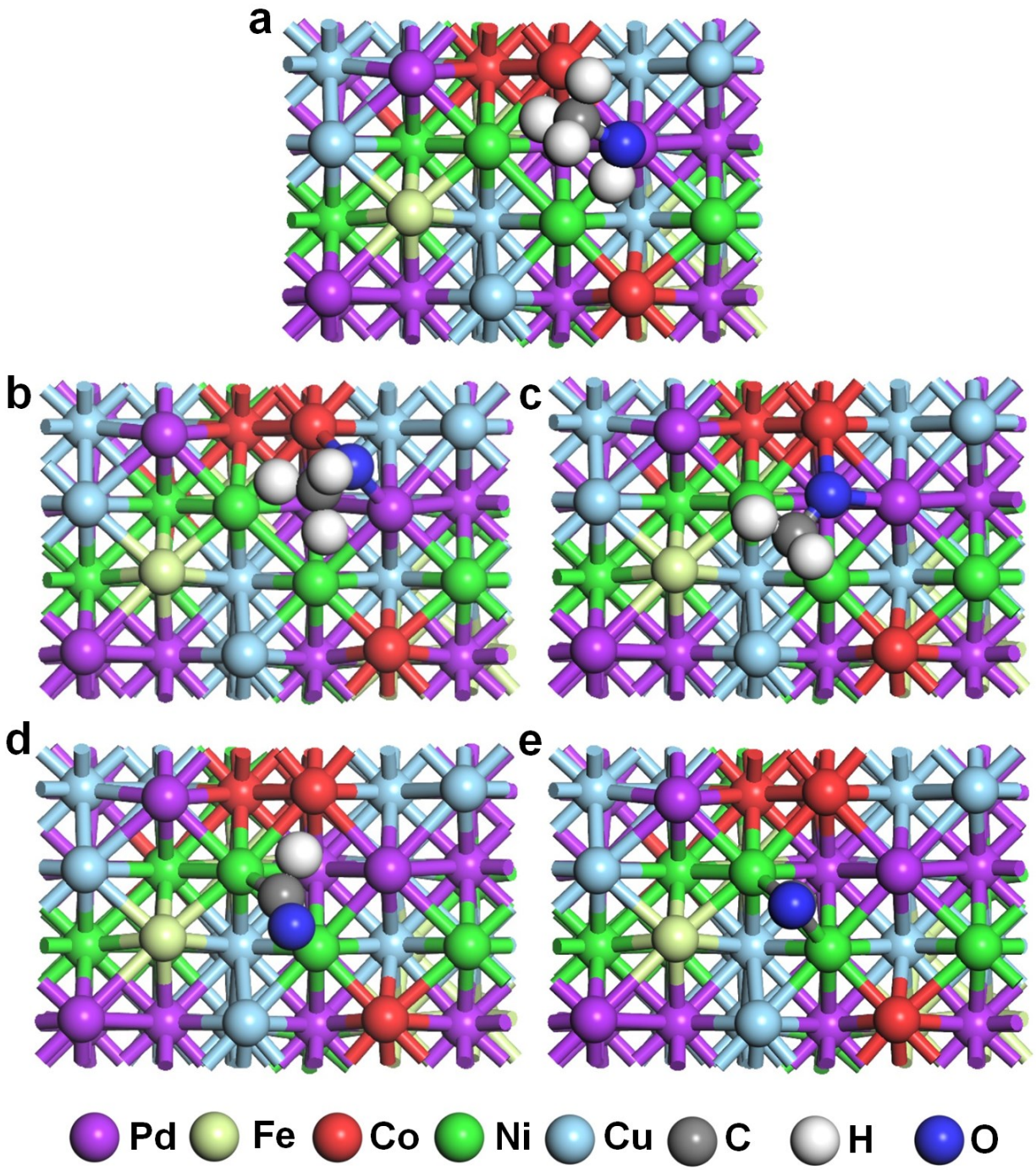

Figure S15. The absorption sites of a) CH_3OH, b) CH_3O, c) CH_2O, d) CHO, and e) CO on PdFeCoNiCu-pHENs.

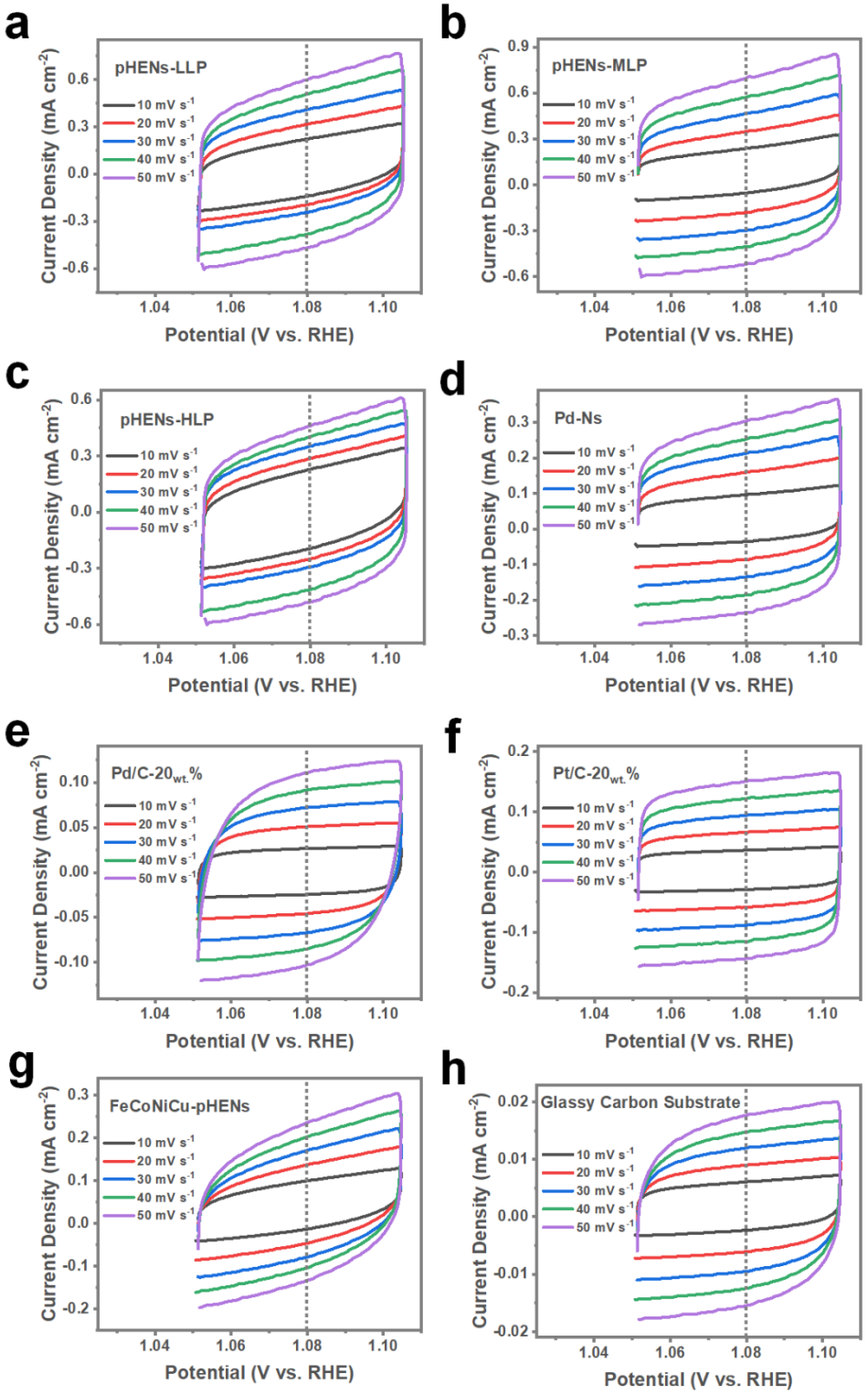

Figure S16. CV curves of a) pHENs-MLP; b) pHENs-LLP; c) pHENs-HLP; d) Pd-Ns; e) Pd/C-20$_{wt.}$%; f) Pt/C-20$_{wt.}$%; g) FeCoNiCu-pHENs; e) Glassy carbon substrate in 1 M KOH solution with various scan rates.

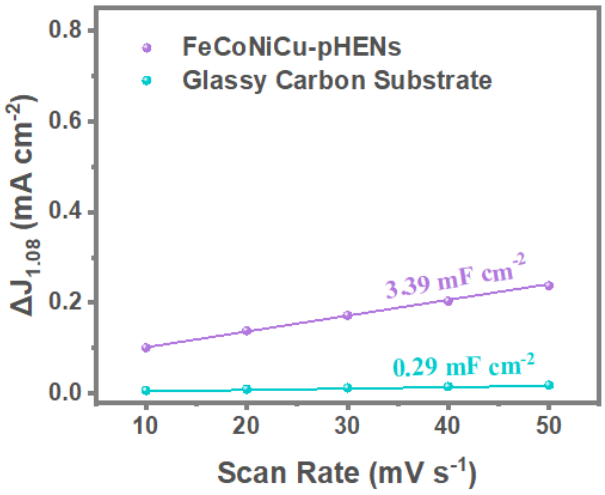

Figure S17. C_{dl} values of FeCoNiCu-pHENs and glassy carbon substrate.

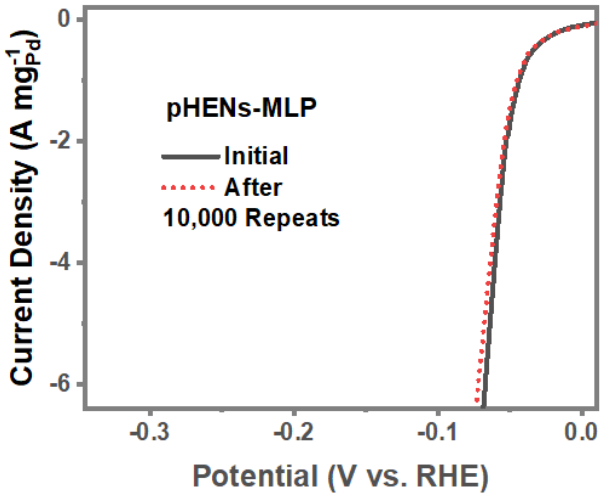

Figure S18. HER mass activity of pHENs-MLP before and after 10,000 times LSV repetitive test.

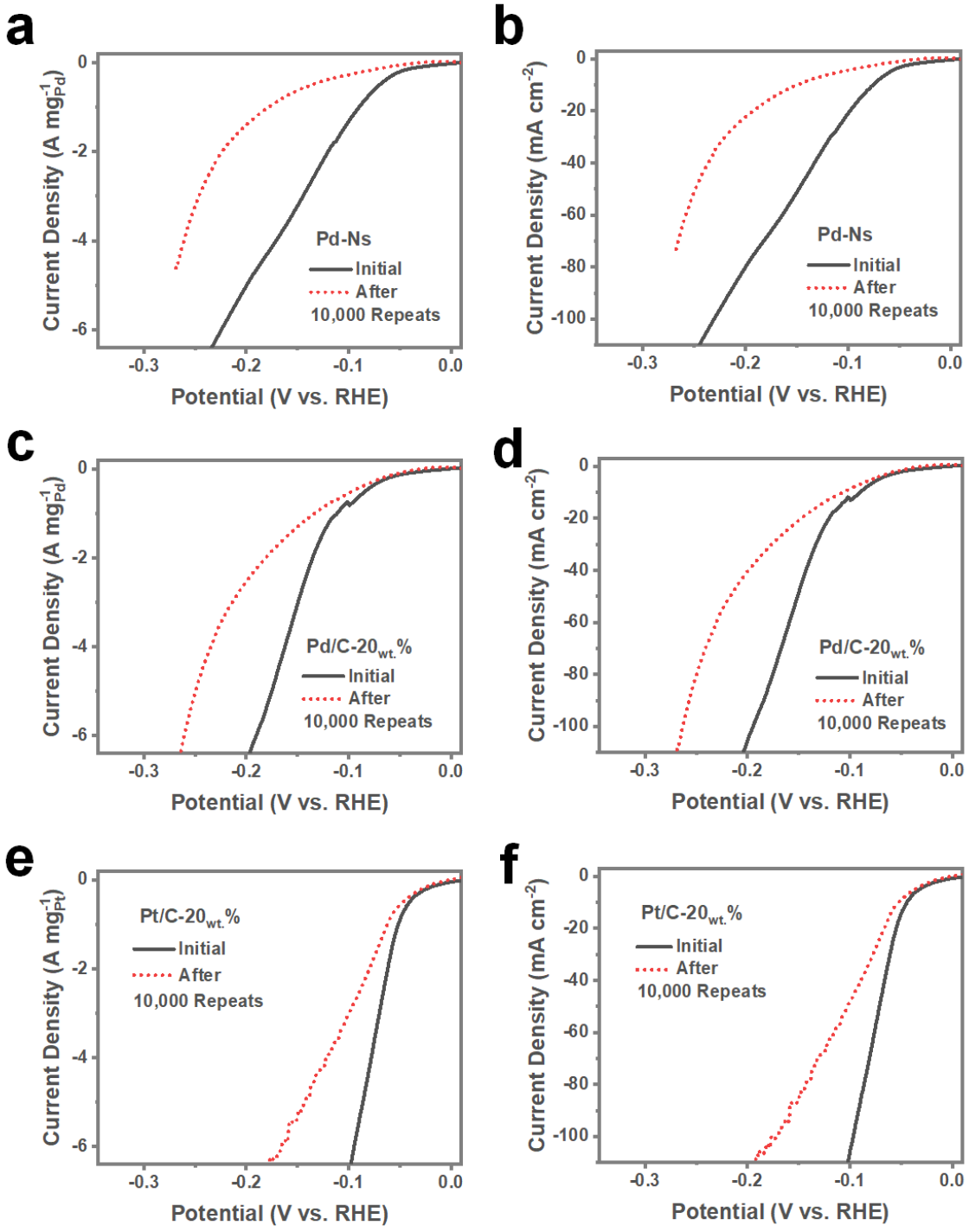

77

78 Figure S19. Electroactivities of contrast samples before and after 10000 repeats HER test. a) Mass and b) specific

79 activity of Pd-Ns; c) Mass and d) specific activity of Pd/C-20$_{wt.}$%; e) Mass and f) specific activity of Pt/C-20$_{wt.}$%.

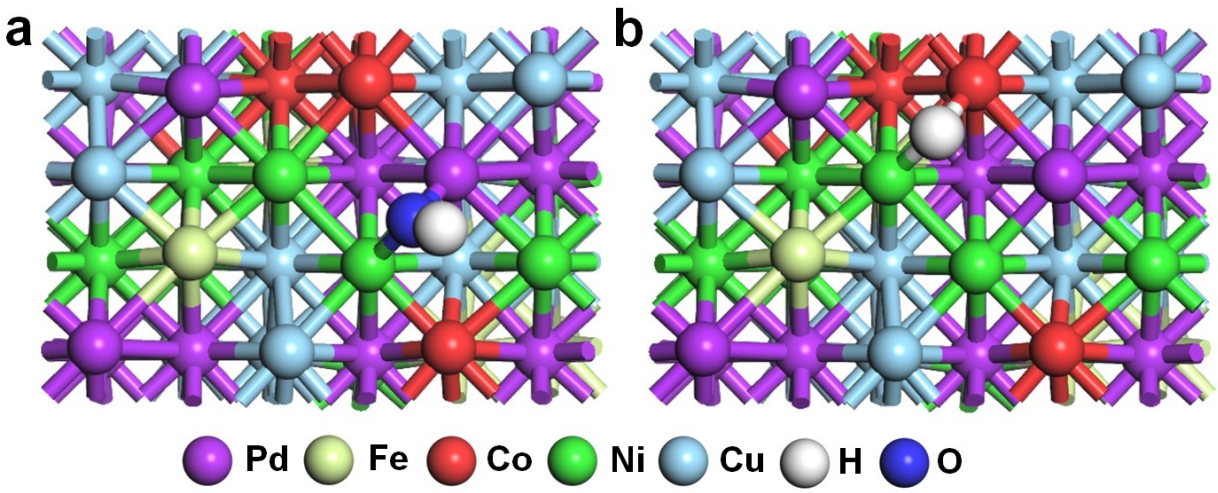

Figure S20. The absorption sites of a) *OH and b) *H on the PdFeCoNiCu-pHENs.

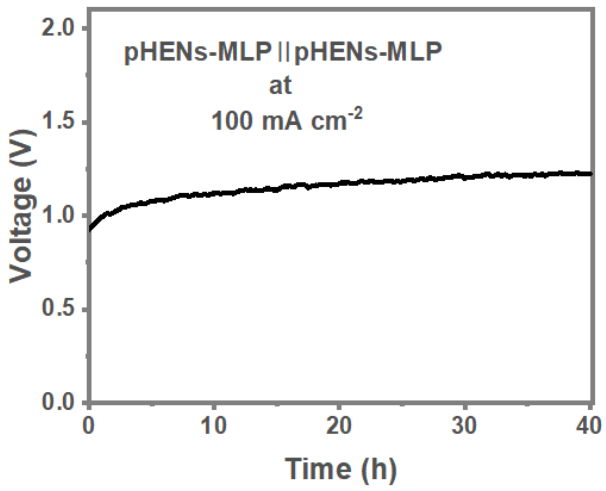

Figure S21. Chronopotentiometry curve of PdFeCoNiCu-pHENs (pHENs-MLP) at a specific current density of 100 mA cm^{-2}.

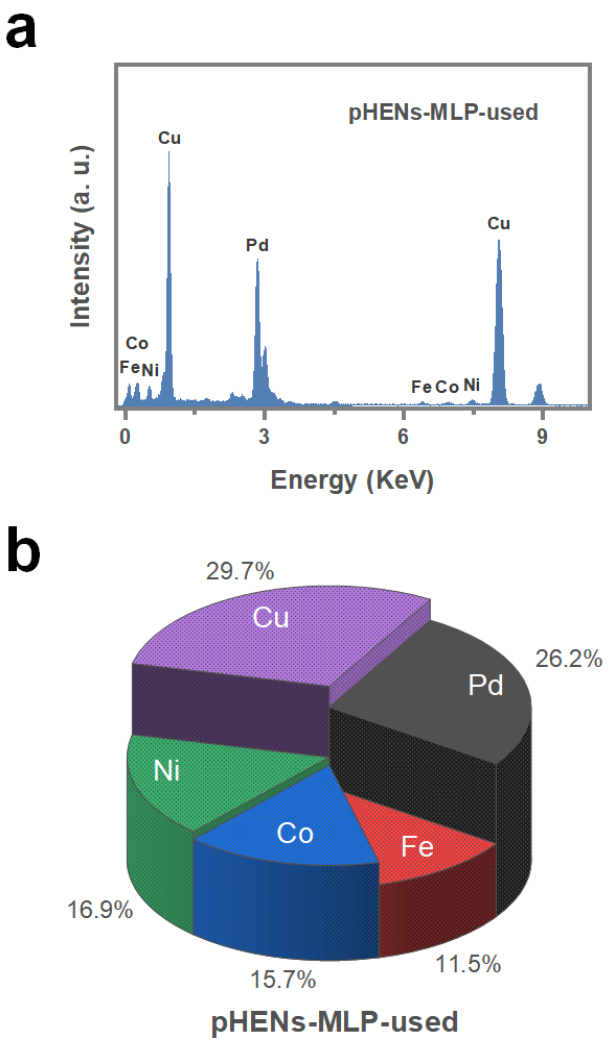

87

88 Figure S22. Element mass ratio of PdFeCoNiCu-pHENs after MOR-assisted hydrogen generation test. a) EDX

89 spectra and b) element mass ratio of PHENs-MLP-used.

90

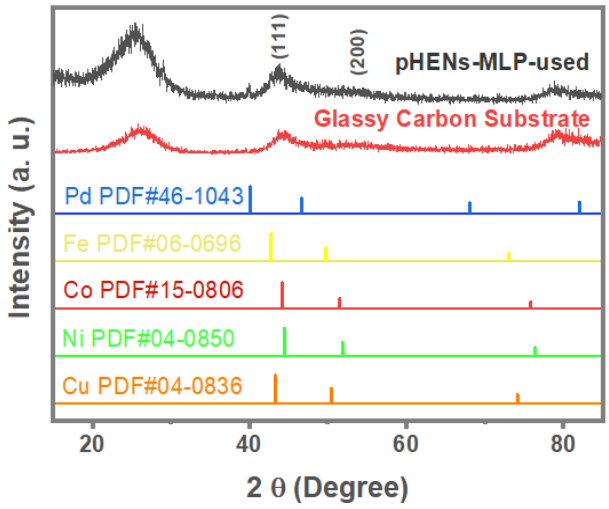

91

92 Figure S23. XRD patterns of the pHENs-MLP-used and glassy carbon substrate.

93

94

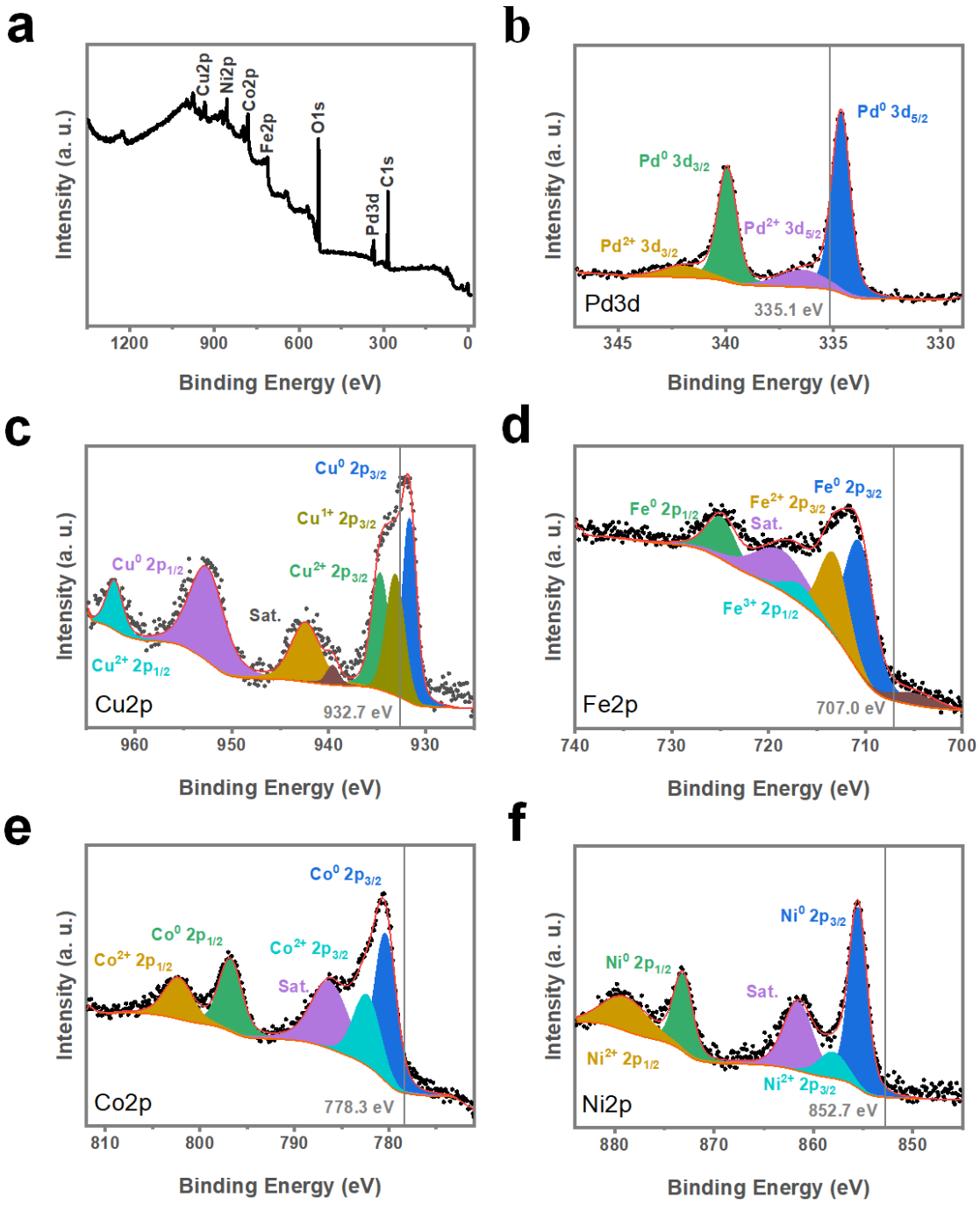

Figure S24. XPS characterization of the pHENs-MLP-used. a) Survey curve; High-resolution XPS spectrums of b) Pd 3d, c) Cu 2p, d) Fe 2p, e) Co 2p, and f) Ni 2p.